A&A 513, A74 (2010)
DOI: 10.1051/0004-6361/200913373

Astronomy & Astrophysics

Another cluster of red supergiants close to RSGC1

I. Negueruela[1], C. González-Fernández[1], A. Marco[1], J. S. Clark[2], and S. Martínez-Núñez[1]

[1] Departamento de Física, Ingeniería de Sistemas y Teoría de la Señal, Universidad de Alicante, Apdo. 99, 03080 Alicante, Spain
e-mail: ignacio.negueruela@ua.es
[2] Department of Physics and Astronomy, The Open University, Walton Hall, Milton Keynes MK7 6AA, UK

Received 29 September 2009 / Accepted 5 January 2010

ABSTRACT

Context. Recent studies have revealed massive star clusters in a region of the Milky Way close to the tip of the Long Bar. These clusters are heavily obscured and are characterised by a population of red supergiants.
Aims. We analyse a previously unreported concentration of bright red stars ∼16′ away from the cluster RSGC1
Methods. We utilised near IR photometry to identify candidate red supergiants and then *K*-band spectroscopy of a sample to characterise their properties.
Results. We find a compact clump of eight red supergiants and five other candidates at some distance, one of which is spectroscopically confirmed as a red supergiant. These objects must form an open cluster, which we name Alicante 8. Because of the high reddening and strong field contamination, the cluster sequence is not clearly seen in 2MASS or UKIDSS near-IR photometry. From the analysis of the red supergiants, we infer an extinction $A_{K_S} = 1.9$ and an age close to 20 Myr.
Conclusions. Though this cluster is smaller than the three known previously, its properties still suggest a mass in excess of 10 000 $M_\odot$. Its discovery corroborates the hypothesis that star formation in this region has happened on a wide scale between ∼10 and ∼20 Myr ago.

Key words. stars: evolution – supergiants – Galaxy: structure – open clusters and associations: individual: Alicante 8

1. Introduction

Over the past few years, the census of massive ($M_{\rm cl} \gtrsim 10^4\ M_\odot$) clusters in the Milky Way has steadily increased, with the discovery of three such clusters near the Galactic centre (Krabbe et al. 1995; Nagata et al. 1995; Cotera et al. 1996; Figer et al. 1999) and the realisation that Westerlund 1 has a mass of the order of $10^5\ M_\odot$ (Clark et al. 2005). Similar clusters are known in many other galaxies and are typical of starburst environments, where they appear in extended complexes (e.g, Bastian et al. 2005). Targeted searches revealed three more massive clusters in a small region of the Galactic plane, between $l = 24°$ and $l = 29°$ (Figer et al. 2006; Davies et al. 2007; Clark et al. 2009a). The Long Galactic Bar is believed to end in this region (Cabrera-Lavers et al. 2008), touching what has been called the base of the Scutum-Crux arm (Davies et al. 2007, from now on D07), which may also be considered a part of the Molecular Ring (e.g., Rathborne et al. 2009).

These three highly-reddened clusters are dominated by large populations of red supergiants (RSGs), which appear as very bright infrared sources, while their unevolved populations have not been yet characterised. RSGC1 is the most heavily obscured, with an estimated $\tau = 12 \pm 2$ Myr and $M_{\rm initial} = 3 \pm 1 \times 10^4\ M_\odot$ (Davies et al. 2008). RSGC2 = Stephenson 2 is the less obscured and apparently most massive of the three, with $\tau = 17 \pm 3$ Myr and $M_{\rm initial} = 4 \pm 1 \times 10^4\ M_\odot$ (D07). Finally, RSGC3 lies at some distance from the other two and has an estimated $\tau = 16$–20 Myr and an inferred $M_{\rm initial} = 2$–$4 \times 10^4\ M_\odot$ (Clark et al. 2009a; Alexander et al. 2009). Collectively, the three clusters are believed to host >50 true RSGs (i.e., $M_{\rm ZAMS} \gtrsim 12\ M_\odot$), the kind of objects thought to be the progenitors of type IIn supernovae (Smartt et al. 2009).

In this paper, we report the discovery of one more cluster of red supergiants in the immediate vicinity of RSGC1, which we designate as Alicante 8 = RSGC4[1]. Identified visually in 2MASS K_S images as a concentration of bright stellar sources near $\ell = 24\overset{\circ}{.}60$, $b = +0\overset{\circ}{.}39$ (see Fig. 1), we utilised near-IR photometry to identify potential cluster members, nine of which were subsequently observed spectroscopically and confirmed to be RSGs. Though this cluster is perhaps less massive than the other three, it provides further evidence for the presence of an extended star formation region in the direction of the end of the Long Bar.

2. Data acquisition and reduction

As discussed by Clark et al. (2009a), it is extremely difficult to determine a physical extent for any of the RSG clusters, since their unevolved populations are not readily visible as overdensities with respect to the field population in any optical or infrared band. In view of this, we must rely on the apparent concentration of bright infrared sources to define a new cluster. In the absence of spectral and/or kinematical information, it is difficult to distinguish between bona fide cluster RSGs and a diffuse field

[1] Though designating this cluster RSGC4 may seem the most natural step, this choice raises the question of when a cluster should be considered a cluster of red supergiants, i.e., how many red supergiants are needed and how prominent the supergiants have to be with respect to the rest of the cluster. For this reason, we favour the alternative names.

Fig. 1. Near-IR *JHK*-band colour composite of the field around Alicante 8, constructed from UKIDSS data with artifacts due to saturation artificially removed and colour enhancement. Note the lack of a clearly defined stellar overdensity of unevolved cluster members with respect to the field. The image covers approximately 5.′5 × 4′.

population (cf. D07). We are thus forced to utilise photometric data to construct a list of candidate cluster members.

2.1. 2MASS data

We have used 2MASS JHK_S photometry to identify the RSG population. Based on the spatial concentration of bright red stars (Fig. 2), we start by taking 2MASS photometry for stars within $r \leq 7'$ of the position of Star 4 (RA: $18^h34^m51.0^s$, Dec: $-07°14'00.''5$), selecting stars with low photometric errors ($\Delta K_S \leq 0.05$). A number of bright stars defining the spatial concentration have very high $(J - K_S) \approx 3.5$ values and form a well-separated clump in the $(J - K_S)/K_S$ diagram (Fig. 3). The clump, which comprises 11 stars, is also very well defined in the $(H - K_S)/K_S$ diagram, centred around $(H - K_S) = 1.2$. We name these stars S1–3 and S5–12.

We make use of the reddening-free parameter $Q = (J - H) - 1.8 \times (H - K_S)$ (see, e.g., Negueruela & Schurch 2007) to estimate the nature of stars. Using, e.g., the intrinsic colour calibration of Straižys & Lazauskaitė (2009), we see that early-type stars must have $Q \lesssim 0.0$, while the dominant population of bright field stars, red clump giants, have $Q \approx 0.4$–0.6. Perhaps because of colour terms and the structure of their atmospheres, most RSGs do not deredden correctly when the standard law is assumed, and give values $Q = 0.1$–0.4. Examination of the fields of the three known RSG clusters shows that more than two thirds of the RSGs give low values of Q (≈0.1–0.3), while the remaining show $Q \approx 0.4$, typical of red stars. No dependence with the spectral type is obvious.

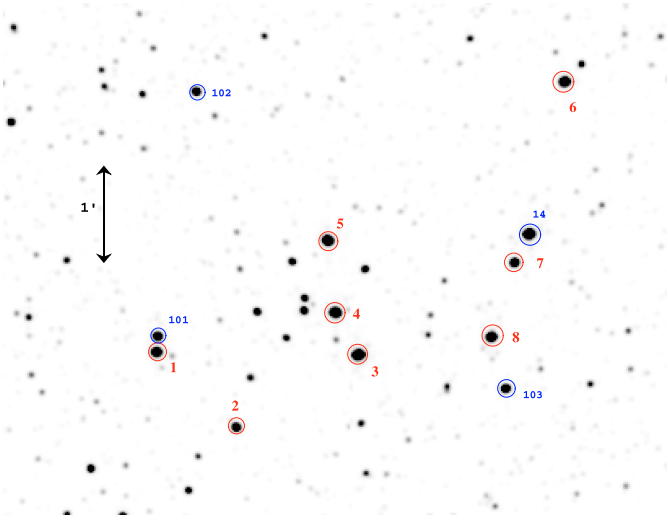

Fig. 2. Finding chart for Alicante 8, with the stars listed in Table 1 indicated. The finder comprises a *K*-band image from 2MASS with a ~7′ × 5′ field encompassing all the confirmed members (S1–8, marked by red circles). Other stars discussed in the text are marked by blue circles.

Table 1. Summary of RSG candidates and their properties[a] .

ID	Co-ordinates		2MASS				GLIMPSE *Spitzer*[c]			*MSX*				Offset
	RA	Dec	J	H	K_S	Q	4.5 μm	5.8 μm	8.0 μm	A	C	D	E	
S1	18 34 58.40	−07 14 24.8	9.92	7.80	6.67	0.10	–	5.54	5.32	5.17	4.48	4.29	–	3.″2
S2	18 34 55.12	−07 15 10.8	10.86	8.45	7.32	0.38	6.73	6.37	6.31	6.07	5.11	5.05	–	2.″1
S3	18 34 50.00	−07 14 26.2	9.55	7.19	6.00	0.22	–	4.84	4.68	4.69	3.57	3.42	3.32	2.″8
S4	18 34 51.02	−07 14 00.5	10.73	7.68	6.14	0.29	–	4.65	4.50	4.45	3.43	3.35	3.02	0.″5
S5	18 34 51.33	−07 13 16.3	10.04	7.53	6.26	0.23	none within 10″			5.00	4.01	3.87	–	1.″5
S6	18 34 41.55	−07 11 38.8	10.26	7.73	6.43	0.18	–	5.30	5.19	5.14	4.49	–	–	2.″7
S7	18 34 43.56	−07 13 29.7	10.46	8.22	7.06	0.13	–	5.94	5.88	none within 10″				
S8	18 34 44.51	−07 14 15.3	10.42:[d]	8.03	6.62	−0.15[d]:	–	4.75	4.63	4.34	3.56	3.18	2.86	0.″7
S9	18 34 45.81	−07 18 36.2	9.83	7.63	6.49	0.14	–	4.99	4.83	4.96	4.48	–	–	1.″7
S10	18 34 26.81	−07 15 27.9	10.98	8.32	7.00	0.29	–	5.78	5.61	5.22	4.12	–	–	0.″9
S11	18 35 00.32	−07 07 37.4	9.61	7.47	6.34	0.11	–	5.35	5.12	4.73	3.69	3.59	2.77	0.″3
S12	18 35 16.88	−07 13 26.9	9.87	7.73	6.45	−0.15	–	4.66	4.45	4.54	3.48	3.31	3.39	0.″5
S13	18 35 10.89	−07 15 17.8	12.14	9.09	7.45	0.11	none within 7″			4.16	3.08	2.81	2.26	1.″0
S14	18 34 42.94	−07 13 12.2	8.60	6.87	6.10	0.35	–	5.53	5.50	5.23	4.69	5.12	1.21	> 6″
S101	18 34 58.36	−07 14 15.1	9.80	7.96	7.19	0.45	–	6.61	6.57	5.17	4.48	4.20	–	> 6″
S102	18 34 56.77	−07 11 44.9	10.36	8.36	7.52	0.49	–	6.83	6.88	7.42	–	–	–	> 9″
S103	18 34 43.92	−07 14 47.0	9.76	8.07	7.34	0.38	6.97	6.79	6.73	none within 10″				
S104	18 35 02.42	−07 09 33.4	10.26	8.40	7.58	0.38	7.22	6.96	6.89	6.53	–	–	–	1.″4
S105	18 35 07.59	−07 18 47.4	10.33	8.36	7.59	0.58	7.13	6.89	6.95	5.06	4.26	5.30	–	5.″9
S106	18 35 06.67	−07 18 55.2	10.15	8.24	7.41	0.42	7.09	6.78	6.82	none within 10″				
S107	18 34 27.37	−07 16 19.1	9.74	7.94	7.10	0.28	6.86	6.53	6.53	5.87	5.34	–	–	3.″1
S108	18 34 28.66	−07 09 57.4	9.94	8.02	7.17	0.15	6.88	6.51	6.52	6.54	–	–	–	1.″3
S109	18 34 50.86	−07 18 11.9	10.45	8.61	7.76	0.31	7.43	7.13	7.11	6.08	–	–	–	5.″1

Notes. Top panel: spectroscopically confirmed RSGs and photometric candidates without spectroscopic observations. Bottom panel: other objects whose photometric properties are indicative of luminous red stars, but are likely to be foreground to the cluster. The last column gives the offset between the star location and the nearest *MSX* source[b] .
[(a)] Co-ordinates and near-IR magnitudes are from 2MASS, with mid-IR (∼4–25 μm) magnitudes from the Galactic plane surveys of GLIMPSE/*Spitzer* (Benjamin et al. 2003) and the *Midcourse Source Experiment (MSX)* (Egan et al. 2001).
[(b)] The nominal positions of *MSX* sources have 1.″5 uncertainties. Offsets much larger than 3″ are then likely to indicate random superpositions.
[(c)] None of the candidate cluster members is detected by *Spitzer* at 3.6 μm.
[(d)] The J magnitude for S8 has quality flag E, indicating a poor fit of the PSF.

Of the 11 stars in the clump, 9 have Q in the typical range for RSGs. One other object, S8 has its J magnitude marked as unreliable in 2MASS, and has therefore an unreliable Q value. The final star, S12, has $Q = -0.15$, indicative of an infrared excess. In addition to these 11 objects, two other stars with Q in the interval typical of supergiants, S4 and S13, have redder $(J - K_S)$ and $(H - K_S)$ colours than the rest. We consider the 11 stars in the clump and these two redder stars as candidate RSGs. Finally, one star S14, has Q typical of supergiants, but much bluer colours, and we do not consider it a candidate cluster member, but a candidate foreground RSG. Stars S1–8 are spatially concentrated and define the cluster core (Fig. 2). Stars S9–13 are located at greater distances, and not shown in Fig. 2. The coordinates and magnitudes of all the stars under discussion are listed in Table 1.

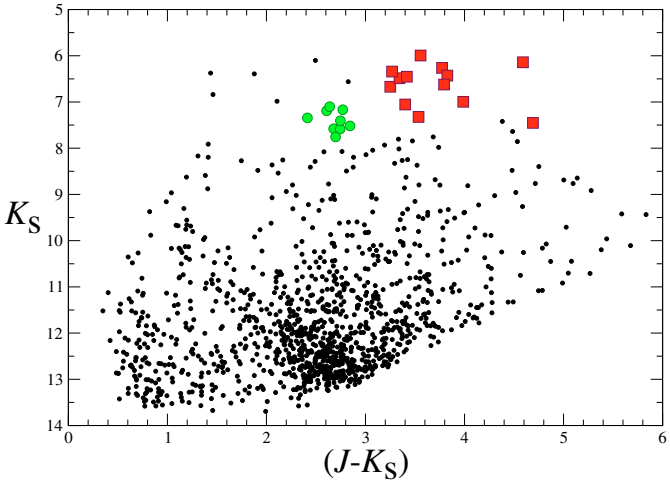

Fig. 3. Colour magnitude plot for stars within 7′ of Alicante 8, using 2MASS data. The likely cluster members identified in Sect. 2.1 are indicated by the red squares, while the group of less luminous objects discussed in Sect. 4 are plotted as green circles. Note that the two stars with $(J - K_S) \sim 4.5$ are S4 and S11 (see text). The former is spectroscopically confirmed as an RSG, but the second is fainter than most members, and requires spectroscopic study.

2.2. Spectroscopy

A sample of the candidates were subsequently observed with the Long-slit Intermediate Resolution Infrared Spectrograph (LIRIS) mounted on the 4.2 m William Herschel Telescope (WHT), at the Observatorio del Roque de los Muchachos (La Palma, Spain). The instrument is equipped with a 1024 × 1024 pixel HAWAII detector. Stars 1, 3–6 and 8 were observed in service mode on the night of June 29, 2009, while stars 2, 7 and 9 were observed during a run on July 6 and 7, 2009. The configuration was the same in both cases. We profited from the excellent seeing to use the 0.″65 slit in combination with the intermediate-resolution K pseudogrism. This combination covers the 2055–2415 nm range, giving a minimum $R \sim 2500$ at 2055 nm and slightly higher at longer wavelengths.

Data reduction was carried out using dedicated software developed by the LIRIS science group, which is implemented

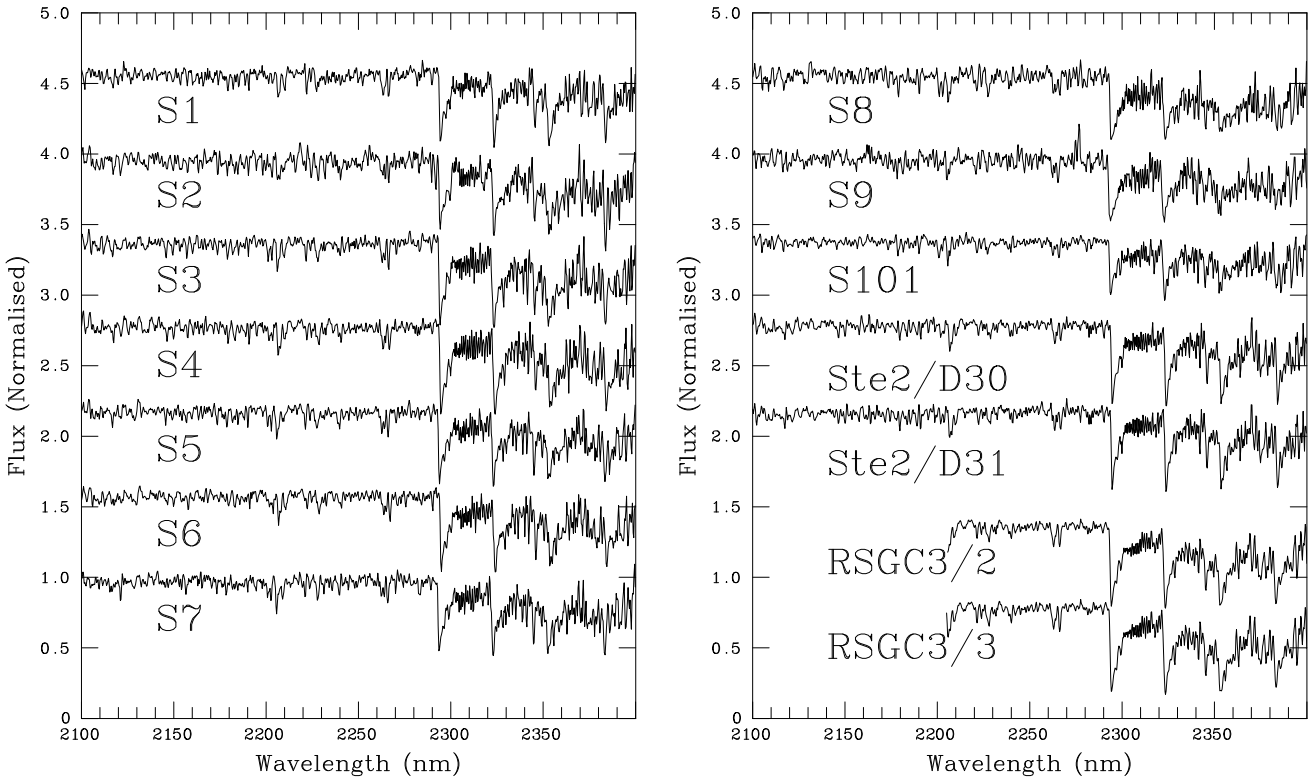

Fig. 4. *Left*: *K*-band spectra of the eight confirmed members in the core of the new cluster, Alicante 8. *Right*: *K*-band spectra of two other stars in the field. S9 is a supergiant at some distance from the cluster, which may well be a member, in spite of slightly lower reddening. S101 is a foreground bright giant coincident with the cluster, part of a population spread over the whole field. As a comparison, we show two RSGs in Stephenson 2 observed with the same setup. We also show two RSGs in RSGC3, observed at similar resolution (Clark et al. 2009a).

within IRAF[2]. We used the A0 V star HIP 90967 to remove atmospheric features, by means of the XTELLCOR task (Vacca et al. 2003). The spectra of all the stars are shown in Fig. 4. We also shown the spectrum of a star which felt by chance inside the slit when observing S1. We call this star S101 and will discuss it further down.

2.3. UKIDSS data

We complete our dataset by utilising UKIDSS *JHK* photometry (Lawrence et al. 2007). The data were taken from the Galactic Plane Survey (Lucas et al. 2008) as provided by the Data Release 4 plus.

3. Results

3.1. Supergiant members

Figure 4 shows the spectra of candidates S1–9, together with that of S101. All the stars observed show deep CO bandhead absorption, characteristic of late type stars. Following the methodology of D07, it is possible to use the equivalent width of the CO bandhead feature, $EW_{\rm CO}$, to provide an approximate spectral classification for the stars.

D07 measure the $EW_{\rm CO}$ between 2294−2304 nm. Unfortunately, at the resolution and signal-to-noise of our spectra, the continuum band defined by D07 does not provide a reliable determination of the continuum. Therefore we choose to select the continuum regions from González-Fernández et al. (2008), with which this value is obtained over a wider range in wavelength and therefore less prone to be tainted by spurious effects. We use the spectra of two confirmed RSGs in Stephenson 2 with magnitudes comparable to our sample (observed with the same setup) to ensure that our *EW*s are measured in the same scale as those of D07. The values measured agree within 1 Å with those determined by D07.

In addition, we profit from the recent publication of the atlas of infrared spectra of Rayner et al. (2009) to verify the calibration of spectral type against $EW_{\rm CO}$ (D07). Thanks to the atlas, we can use a much higher number of M-type stars than in the original calibration and extend it to later spectral types. We measure $EW_{\rm CO}$ by defining the same continuum regions as used for our targets. The results are plotted in Fig. 5.

In the plot, we have used all the giants and supergiants with spectral type between G0 and M7, leaving out a few early G objects with no measurable CO bandhead. We have also included giants with spectral type M8–9. For G and K stars, our results reproduce very well those of D07. Supergiants and giants appear well separated, with a few exceptions. Some of the exceptions are due to spectral variability. For instance, two of the three supergiants falling close to the position of the giants are known spectral type variables (RW Cep and AX Sgr), and have not been used for the fit. The two giants falling along the location of the supergiants have luminosity class II. Most objects with luminosity class II have higher $EW_{\rm CO}$ than luminosity class III objects of the same spectral type, but only these two stand out strongly.

For the M stars, the situation is not so clear. At a given spectral type, there is very significant scatter in the values of $EW_{\rm CO}$,

[2] IRAF is distributed by the National Optical Astronomy Observatories, which are operated by the Association of Universities for Research in Astronomy, Inc., under cooperative agreement with the National Science Foundation

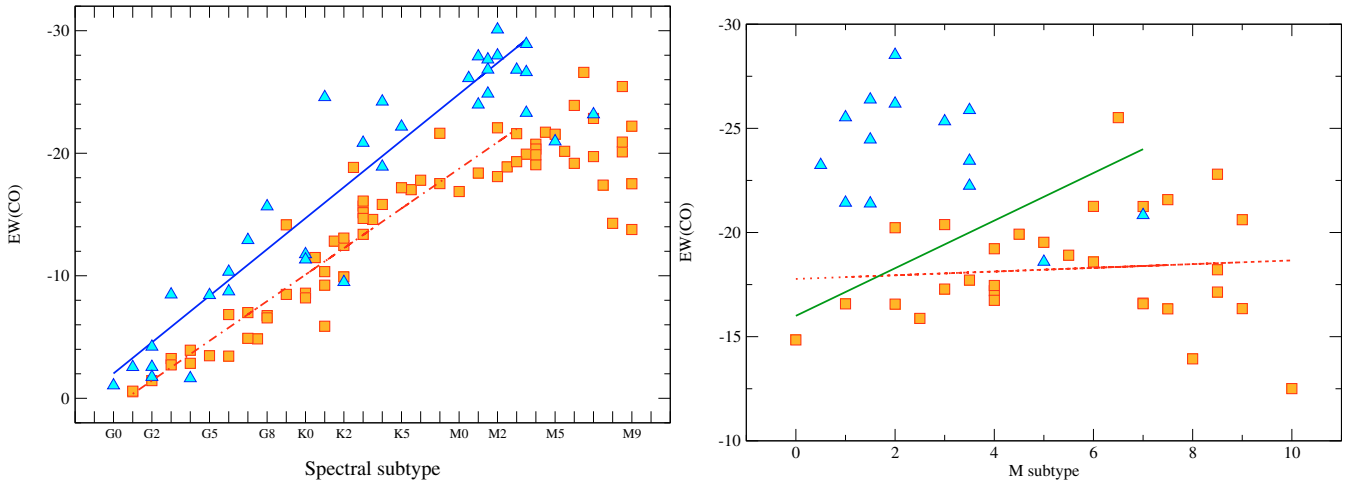

Fig. 5. *Left panel*: relationship between spectral type and the equivalent width of the CO bandhead for G–M type stars in the catalogue of Rayner et al. (2009). Giants are plotted as squares while supergiants are triangles. The continuous line is a fit to all the supergiants between G0 and M3, with the exception of two spectrum variables mentioned in the text. The dot-dashed line is the fit to all giants between G0 and M3. *Right panel*: same for only the M-type stars in the catalogue of Rayner et al. (2009), including some Mira-type spectrum variables which were excluded from the left panel. The dotted line represents the best fit to the data for all the M-type giants, while the continuous line is the fit by D07 to giants in the range G0 to M7.

especially for supergiants, but also for very late giants. Most supergiants have higher EW_{CO} than most giants, but there are a few exceptions in both directions. This is, in part, not so surprising, because some AGB stars are as luminous as some supergiants (van Loon et al. 2005). Our sample almost completely lacks supergiants later than M4. The apparent lack of correlation between EW_{CO} and spectral type for M supergiants is partly due to the position of the M5 Ib–II star HD 156014, which has a very low luminosity, and is the only supergiant in the range. As D07 have several supergiants with spectral types >M4, we will accept their calibration in this range.

Our data show that the slope of the relationship does not keep constant for giants with spectral type ≥M5, as these objects do not show, on average, higher values of EW_{CO} than the earlier M giants. This is comforting, as it supports the assumption – based on the calibration of D07 – that any star with $EW_{CO} > 24$ Å is almost certainly a supergiant, and that any star with $EW_{CO} \gtrsim 22$ Å is very likely a supergiant.

Turning back to our targets, S101, which was not selected as an RSG candidate, shows $EW_{CO} = 18$ Å, a value typical of M giants. All the other stars have higher equivalent widths, in the region of supergiants. In particular, stars S3, S4, S6, S8 and S9 have $EW_{CO} > 24$ Å, and must be RSGs according to the calibration of D07. The other four stars have 21Å $< EW_{CO} < 24$ Å and can be either K supergiants or M giants. Of them, only S2 has a Q value compatible with being a red giant. Based on this, we assume that all the candidates are supergiants, though noting that S2 could be a giant.

As discussed, we use the calibration of D07 to estimate spectral types for the confirmed supergiants. The derived types, which must be considered approximate because of the procedure used (D07 estimate uncertainties of ±2 subtypes), are listed in Table 2. Interestingly, S4, which has the redder colours, also has the deepest CO bandhead, indicative of a spectral type M6 I. Though the spectral types are approximate, the distribution is not very different from the other RSG clusters, with types extending from K4 I to M6 I. We note that there seems to be some tendency for lower mass RSGs to have spectral type K (Humphreys & McElroy 1984; Levesque et al. 2005).

Table 2. Summary of the stellar properties of the 9 RSGs for which spectral classification was possible.

ID	Spec type	$T_{\rm eff}(K)^a$	$(J-K)_0$	$(J-K)$	$E(J-K)$	$A_K{}^c$	$M_K{}^{c,d}$
S1	K5 I	3840 ± 135	0.75	3.25	2.50	1.68	−9.1
S2	K4 I	3920 ± 112	0.72	3.54	2.82	1.89	−8.7
S3	M3 I	3605 ± 147	0.90	3.56	2.66	1.78	−9.9
S4	M6 I	3400 ± 150	1.05^b	4.59	3.54	2.37	−10.3
S5	K5 I	3840 ± 135	0.75	3.77	3.02	2.02	−9.9
S6	M2 I	3660 ± 127	0.87	3.83	2.96	1.98	−9.7
S7	K5 I	3840 ± 135	0.75	3.40	2.65	1.78	−8.8
S8	M2 I	3660 ± 127	0.87	3.79	2.92	1.94	−9.4
S9	M1 I	3745 ± 117	0.85	3.34	2.49	1.67	−9.3

Notes. [a] Assumed from the calibration of Levesque et al. (2005), following Davies et al. (2008); [b] extrapolated from the calibration; [c] typical errors in A_K and M_K are 0.2 mag (see text for discussion); [d] assuming a distance of 6.6 kpc, identical to RSGC1.

Further, we calculate the Q value for all the stars in the atlas of Rayner et al. (2009), finding that almost all K and M-type giants have $Q \approx 0.4$–0.6, with the exception of Miras, which have $Q < 0$ because of the colour excess caused by their dust envelopes. This also supports a supergiant nature for all our likely members (S2 may still be a red giant, but it falls together with the other members in the photometric diagrams).

The eight candidates in the central concentration are very likely all RSGs, and thus we take them as cluster members, even in the absence of kinematic data. Of the halo candidates, we have only observed S9. This object is slightly less reddened than the confirmed members. As seen in Fig. 4, its morphology resembles more closely that of S101 than those of the confirmed RSGs. However, the measured $EW_{CO} = 25$ Å indicates that this object must definitely be a supergiant, though we cannot confirm its membership, as we lack kinematic data.

Interestingly, Table 1 shows that, amongst the confirmed RSGs, the three stars with late spectral types are the only ones detected in all MSX bands, though their dereddened [A − C] colours do not provide immediate evidence for colour

excesses indicative of a large dust envelope. (cf. D07). However, the very high $E(J-K_S)$ and $E(H-K_S)$ colours of S4, suggest intrinsic extinction, indicative of circumstellar material.

3.2. Reddening and age

The lack of kinematic data also complicates a determination of the distance to the cluster. RSGs span a wide range of luminosities ($\log(L_{bol}/L_\odot) \sim 4.0-5.8$; Meynet & Maeder 2000), and therefore absolute magnitudes cannot be inferred from the approximate spectral types. In addition, the extinction in this direction is very high. Davies et al. (2008) derive $A_{K_S} = 2.6$ for the nearby RSGC1. We make a quick estimation of the reddening to Alicante 8 by using the intrinsic colours of RSGs from Elias et al. (1985). We take the values for luminosity class Iab stars, but, considering the huge values of the reddening and the uncertainty in the spectral type, this choice is unlikely to be the main contributor to dispersion. We note that the intrinsic colours of Elias et al. (1985) are in the CIT system, but again this effect is unlikely to result in a major contribution to dispersion. Individual values are listed in Table 2.

The main source of errors in the calculation of A_K (and so M_K) is the uncertainty in the spectral type calibration from EW_{CO}, which D07 estimate at ±2 subtypes. This value is high enough to allow neglecting the uncertainty in the actual value of EW_{CO}. Rather than propagating this uncertainty through the calculations, we evaluate the total error by constructing a simple Monte Carlo simulation. For a given set of supergiants, with intrinsic colors taken from Elias et al. (1985), we draw extinctions in the K band from a normal distribution $N(\mu, \sigma) = (2, 0.5)$, representative of the expected range for our observations, and use them to calculate their reddened colours and magnitudes. We assign to each of this mock stars an "observed" spectral type (i.e., their real spectral type plus or minus the expected 2 subtypes). With the correspondent intrinsic colour, we invert the equations to obtain a value for A_K and, from it, the corresponding M_K. With this procedure, we estimate that the error in the spectral types translates into a ±0.15 difference in A_K, using a single colour, and 0.1 when averaging the extinction derived from $(H-K_S)$ and $(J-K_S)$. Adding in quadrature the typical errors in the observed colours (0.05 mag) and in the intrinsic colour (0.05 mag), we reach a final figure of ±0.2 mag for every individual determination of M_K.

We find averages $E(J-K_S) = 2.7 \pm 0.2$ and $E(H-K_S) = 1.02 \pm 0.07$, where the errors represent the dispersions in the individual values. We exclude S4 from this analysis, as its $(J-K_S)$ is almost one mag higher than those of all other stars, likely indicative of intrinsic extinction. We also exclude S8, as its 2MASS J magnitude is marked as unreliable, though the values obtained for this star are fully compatible with the others and including it does not change the averages significantly.

The ratio of colour excesses $E(J-K)/E(H-K) = 2.7$ is fully compatible with the standard extinction law (e.g., 2.8 in Indebetouw et al. 2005). These values translate into $A_{K_S} = 1.9 \pm 0.2$, where the uncertainty reflects the dispersion in individual values and the slight difference between the values derived from $E(J-K)$ and $E(H-K)$. The reddening is thus lower than towards RSGC1, but higher than towards the other two RSG clusters in the area.

We can obtain a firm estimate of the distance to the cluster by studying the distribution of interstellar extinction in this direction. For this, we utilise the population of red clump giants (with spectral type K2 III), following the technique of Cabrera-Lavers et al. (2005). This population is seen in the colour–magnitude diagrams as a well defined strip. In the UKIDSS data, we select the giant population within 20′ from Star 4, obtaining the results shown in Fig. 6. This radius is chosen in order to keep the (d, A_K) curve representative for the cluster sightline, while providing a number of stars high enough to permit a proper calculation. Decreasing this value to, for example, 10′ produces noisier results, but does not change the overall behaviour of the extinction. As it is clearly seen, most of the extinction along this sightline arises in a small region located at $d \approx 5$ kpc. The values of A_K measured for Alicante 8 place the cluster at a higher distance, behind the extinction wall, $\gtrsim$6 kpc.

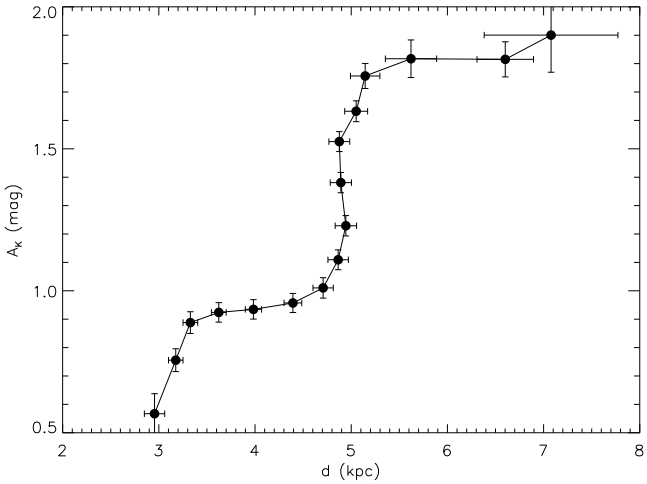

Fig. 6. Run of the extinction in the direction to Alicante 8. The data have been obtained by applying the technique of Cabrera-Lavers et al. (2005) to the red clump giant population within 20′ from S4. The sudden increase in the reddening at ∼ 5 kpc provides a strong lower limit to the distance to the cluster.

Red supergiants in RSGC1 span $K_S = 5.0-6.2$. Those in Alicante 8 cover the range $K_S = 6.0-7.1$ (reaching $K_S = 7.4$ if candidate S13 is confirmed as a member). The range in magnitudes is approximately the same, but the stars are one magnitude fainter. If we take into account that the extinction is higher towards RSGC1, we find that the dereddened magnitudes for stars in Alicante 8 are ∼1.8 mag fainter than those in RSGC1. Given the very high extinction in this region, the possibility that Alicante 8 is significantly more distant than RSGC1 looks very unlikely. Both the distribution of stars in Fig. 3 and the lack of reliable points for $d \gtrsim 7$ kpc in Fig. 6 suggest that the reddening reaches very high values at the distance of the cluster. This rise in extinction could be associated to the presence of molecular clouds in the Molecular Ring. We must thus conclude that the RSGs in Alicante 8 are considerably less luminous than those in RSGC1. Indeed, if we assume a distance $d = 6.6$ kpc, that found for RSGC1 (Davies et al. 2008), we find absolute M_K magnitudes ranging from −8.7 to −10.3. This range is directly comparable to that seen in RSGC3, and implies an age of 16–20 Myr for Alicante 8, the age found for RSGC3 (Clark et al. 2009a)[3], as opposed to the ∼12 Myr for RSGC1 (Davies et al. 2008).

To confirm the age derivation, we plot in Fig. 7 the locations of the RSGs in the theoretical H-R diagram. For this, we follow the procedure utilised by D07. Using the individual extinctions measured above, we derive absolute M_{K_S} magnitudes for the

[3] Note that Alexander et al. (2009) derive a slightly older age (18–24 Myr) for RSGC3, based on a fit to isochrones for non-rotating stellar populations by Marigo et al. (2008). The difference is most likely due to the extinction laws assumed.

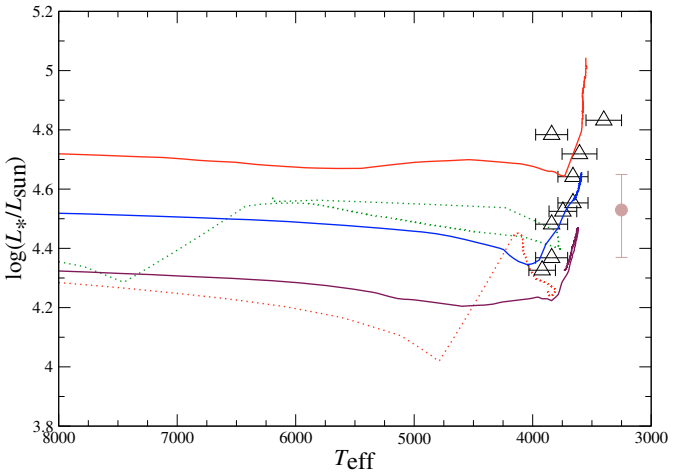

Fig. 7. H-R diagram showing the locations of 8 RSGs at the cluster centre, with their positions derived from the spectral classification, assuming a distance to the cluster d = 6.6 kpc. We also plot isochrones from Meynet & Maeder (2000). The solid lines are the $\log t$ = 7.20 (16 Myr; top, red), $\log t$ = 7.30 (20 Myr; middle, blue) and $\log t$ = 7.40 (24 Myr; bottom, black) with high initial rotation. The dotted lines are the $\log t$ = 7.15 (14 Myr; top, green) and $\log t$ = 7.20 (bottom, red) isochrones without rotation. Errors in $\log L_*$ due to observational uncertainties and calibration issues are small when compared to the uncertainty in the cluster distance ($\Delta D_{\rm cl}$); representative error-bars assuming an uncertainty of ±1 kpc are indicated to the right of the figure.

stars, assuming a distance modulus DM = 14.1 (d = 6.6 kpc). We then use the effective temperature calibration and bolometric corrections of Levesque et al. (2005) to derive $T_{\rm eff}$ and L_* for each object[4]. In Fig. 7, we also plot different isochrones corresponding to the models of Meynet & Maeder (2000). The observational temperatures and luminosities of the RSGs are bound by the $\log t$ = 7.30 (20 Myr) isochrone for stars without rotation and the $\log t$ = 7.15 (14 Myr) isochrone with high initial rotation ($v_{\rm rot}$ = 300 km s^{-1}). As stars in the cluster are likely to have started their lives with a range of rotational velocities, the data are consistent with an age in the 16–20 Myr range. Reducing the distance to the cluster to the nominal 6 kpc adopted by Clark et al. (2009a) for RSGC3 results in a slight increase of age. In this case, the luminosities of some RSGs are marginally consistent with the high rotation $\log t$ = 7.40 (24 Myr) isochrone, though the brightest RSGs seem incompatible with this age.

3.3. The sightline

The stellar population in the direction to Alicante 8 is very poorly known. The Sagittarius Arm is very sparsely traced by the open clusters NGC 6649 (ℓ = 21.°6), NGC 6664 (ℓ = 24.°0) and Trumpler 35 (ℓ = 28.°3). The reddening to these three clusters is variable, but moderate, with values $E(B-V) \approx 1.3$ for Trumpler 35 and NGC 6649 (Turner 1980; Majaess et al. 2008). The reddening law is compatible with standard (R = 3.0) over the whole area (Turner 1980). Around ℓ = 28°, Turner (1980) found several luminous OB supergiants with distances in excess of 3 kpc and reddenings $E(B-V) \approx 1.3$, corresponding to A_K = 0.4. This agrees with our determination of A_K = 0.5 at d = 3 kpc. The reddening increases steeply between 3 and 3.5 kpc, the expected distance for the Scutum-Crux Arm. It then remains approximately constant until it suffers a sudden and brutal increase around d = 5 kpc.

As mentioned above a bright star not selected as a candidate member, S101, fell by chance in one of our slits and turns out to be a luminous red star, though not a supergiant. Examination of the 2MASS CMDs shows that it is part of a compact clump of bright stars, which have been marked as green circles in Fig. 3. These objects, labelled S101–109, are clearly clumped in both the $(J-K_{\rm S})/K_{\rm S}$ and $(H-K_{\rm S})/K_{\rm S}$ diagrams, at much brighter magnitudes than the field population of red clump giants, but are uniformly spread over the field studied. We list their magnitudes in Table 1. These stars are too bright to be red clump stars at any distance. Indeed, their average $(J-K)$ = 2.7 means that, even if they are late M stars, they must be located behind $A_K \sim 1.0$. In view of this, they could be a population of luminous M giants in the Scutum-Crux Arm, implying typical $M_K \approx -6$. They can also be located at the same distance as the extinction wall, but then would have $M_K \lesssim -7$, approaching the luminosity of the brightest AGB stars (van Loon et al. 2005).

Cross correlation with the DENIS catalogue shows that these objects are all relatively bright in the I band, while cluster members are close to the detection limit (with $I \sim 17$) or not detected at all. These again suggests that this population of red giants is closer than the cluster, favouring the Scutum-Crux Arm location. Interestingly, none of these objects has a clear detection in the *MSX* catalogue (Table 1), again confirming their lower intrinsic luminosity.

3.4. The cluster against the background

Unfortunately, we cannot find the sequence of unevolved members for Alicante 8 in either 2MASS or UKIDDS photometry. In this respect, it is worth considering the properties of the open cluster NGC 7419, which contains five RSGs and, though moderately extinguished, is visible in the optical. The 2MASS colour–magnitude diagram for NGC 7419 does not show a well defined sequence, in spite of the fact that the field contamination is very small at the magnitudes of the brightest blue members (Joshi et al. 2008). This is due to differential reddening and the presence of a significant fraction of Be stars amongst the brightest members, which show important colour excesses. With the much higher extinction and field contamination of Alicante 8, its unevolved sequence would be most likely undetectable.

However, we carry out some further tests in order to verify our conclusions. First, we try to estimate the likelihood that the overdensity associated with the cluster may be the result of a random fluctuation. This is very difficult to evaluate, given the very red colours of the stars. The r = 3′ circle centred on S4 shows a clear overdensity of bright stars with respect to the surrounding field. The significance of this overdensity depends very strongly on the set of parameters we use to define the comparison population: we could choose just "bright" stars (i.e., K < 7) or add some extra criteria, such as very red colours (e.g., $(J-K)$ > 2) or Q incompatible with a red clump giant (Q < 0.4). Depending on the criteria selected, the r = 3′ circle presents an overdensity by a factor 2–3 with respect to the surrounding (<1°) field. The existence of the cluster, however, is defined by the presence of a very well defined clump of bright stars in the $Q/K_{\rm S}$, $(H-K_{\rm S})/K_{\rm S}$, and $(J-K_{\rm S})/K_{\rm S}$ diagrams, which no other nearby r = 3′ circle seems to present.

[4] We note that consistency would perhaps demand that we use the intrinsic colours from Levesque et al. (2005), but we prefer to use the same methodology as D07 in order to ease comparison. Using the colours of Levesque et al. (2005) reduces the extinction $A_{K_{\rm S}}$ by ∼0.2 mag, correspondingly decreasing $M_{K_{\rm S}}$ by slightly more than 0.1 mag, too small a difference for any significant impact on the parameters derived.

The possibility that Alicante 8 represents a random overdensity of RSGs seems extremely unlikely in view of the rarity of these objects. In order to consider this option, we would have to assume that most stars with $K_S < 7.5$ in the surrounding field are RSGs, leading to a population of hundreds of RSGs for each square degree. The only other possibility of a random fluctuation would be the random coincidence of a small cluster of RSGs with a number of luminous M giants that happen to have the same colours. This also seems very unlikely. The mid-IR colours of all our candidate supergiants suggest that they are not surrounded by dust. If any ot them were M giants without dusty envelopes, their colours would be only a few tenths of a magnitude redder than those of K supergiants, meaning that they would still be highly reddened and should be placed behind the reddening wall at $d \approx 6$ kpc. Though some AGB stars can reach very bright magnitudes ($A_K \lesssim -8$; van Loon et al. 2005), these are very rare objects (e.g., Groenewegen et al. 2009, for the Magellanic Clouds), descended only from the most massive intermediate-mass stars (Marigo & Giradi 2008). Therefore such a chance coincidence looks equally unlikely.

4. Discussion

The data available reveal that Alicante 8 is a new highly reddened open cluster in the same area where three others had already been located. This discovery represents further evidence for the existence of intense star formation in the region between Galactic longitude $\ell = 24°-28°$. Sightlines in this direction are believed to cross the Sagittarius Arm, cross through the Scutum Arm and then hit the Long Bar close to its intersection with the base of the Scutum Arm at $\ell \sim 27°$, at an estimated distance of ~6.5 kpc.

This coincidence strongly suggests that the tip of the Bar is dynamically exciting star formation giving rise to a starburst region (see discussion in Davies et al. 2007; Garzón et al. 1997). If we take into account the spatial span covered by the four clusters known, this would be by far the largest star-forming region known in the Milky Way.

An alternative view, based on the distribution of molecular clouds in radio maps, is that a giant Molecular Ring is located at the end of the Bar, at a distance ≈4.5 kpc from the Galactic Centre. In this view, our sightline would be cutting through the Ring. We would then be looking through the cross section of a giant star-forming ring, coincident with the Molecular Ring seen in the radio. between distances ~5 and ~8 kpc from the Sun. In this case, the clusters could be spread in depth over a distance ~3 kpc, and not necessarily be associated. As the unevolved population of Alicante 8 cannot be detected, an estimation of its distance will have to wait for data that can provide dynamical information. Meanwhile, we will stick to the assumed 6.6 kpc.

Likewise, a direct estimate of the cluster mass cannot be made. Recent simulations of stellar populations with a Kroupa IMF (Clark et al. 2009b) indicate that a population of 10 000 $M_\odot$ at 16−20 Myr should contain 2−5 RSGs. Cruder estimates using a Salpeter IMF, like those in Clark et al. (2009a), suggest 8 RSGs for each 10 000 $M_\odot$. Therefore, based on the membership of at least 8 RSGs, we can estimate that Alicante 8 contains a minimum of 10 000 $M_\odot$ and, if some of the candidates outside the core are confirmed, could approach 20 000 $M_\odot$. Thus, it seems that it is between half and one third the mass of RSGC2 and RSGC3, which have similar ages, and may be one of the ten most massive young clusters known in the Galaxy.

It is thus quite significant that Alicante 8 does not stand out at all in GLIMPSE mid-IR images, and is only moderately conspicuous over the crowded field in near-IR images. As a matter of fact, the cluster would not appear evident to the eye were it not for the presence of a few foreground objects which, fortuitously, make the clumping of bright stars more apparent (Fig. 1).

In the presence of such a rich foreground (and likely background) population, the detection of massive clusters, even if they are moderately rich in red supergiants, may be a question of chance coincidence with a void in the distribution of bright foreground stars or a hole in the extinction. In this respect, it is worth noting that RSGC1 stands out because of its youth (and hence the intrinsic brightness of its RSGs), while Stephenson 2, apart from being extraordinarily rich in RSGs, is located in an area of comparatively low extinction.

Alicante 8 is located ≈16′ away from RSGC1. If the two clusters are located at a common distance of 6.6 kpc, this angular separation represents a distance of 31 pc, consistent with the size of cluster complexes seen in other galaxies (Bastian et al. 2005). Even if Stephenson 2 (which would be located at ~100 pc from RSGC1 in the opposite direction to Alicante 8) is also physically connected, the distances involved are not excessive. The inclusion of RSGC3, located at 400 pc, in the same starburst region is more problematic, requiring it to be a giant star-formation region. At such distance, the possibility of triggered star formation (in any direction) seems unlikely, but large complexes may form caused by external triggers, as is likely the case of W51 (Clark et al. 2009b; Parsons et al., in preparation).

López-Corredoira et al. (1999) have reported the existence of a diffuse population of RSGs in this area, while D07 detect several RSGs around Stephenson 2 with radial velocities apparently incompatible with cluster membership. Therefore the actual size of the star forming region still has to be determined. The age difference between Alicante 8 and RSGC1 is small, but the Quartet cluster, with an age between 3 and 8 Myr is also located in the same area (about 20′ due East from Alicante 8), at about the same distance (Messineo et al. 2009). Relatively wide age ranges (~5 Myr) are common in cluster complexes. Examples are the central cluster in 30 Dor and its periphery (Walborn et al. 2002) or the several regions in W51 (Clark et al. 2009b).

We have searched for other objects of interest in the immediate vicinity of Alicante 8, but no water masers or X-ray sources are known within 10′ of the cluster. The lack of young X-ray binaries, though not remarkable over such a small area, becomes intriguing when the whole area containing the RSG clusters is considered (cf. Clark et al. 2009a).

5. Conclusions

Alicante 8 contains at least 8 RSGs. If a distance of 6.6 kpc, common to the other RSGCs, is assumed, its age is 16−20 Myr. The presence of these 8 RSGs would then imply a mass in excess of 10 000 $M_\odot$, which could approach 20 000 $M_\odot$ if the candidate members are confirmed.

The discovery of a fourth cluster of red supergiants in a small patch of the sky confirms the existence of a region of enhanced star formation, which we will call the Scutum Complex. As the properties of the four known clusters do not rule out the presence of many other smaller clusters, we are faced with the issue of determining the true nature and extent of this complex. Assuming a common distance for all clusters results in a coherent picture, as they are all compatible with a narrow range of ages (between ~12 and ~20 Myr), showing a dispersion typical of star-forming complexes. However, the spatial extent of this complex should be several hundred parsecs, rising

questions about how such a massive structure may have arisen in our Galaxy.

Further spectroscopic studies, combined with precise radial velocity measurements, will be necessary to confirm the membership of candidate RSGs in the field of Alicante 8 and provide a better estimate of its mass. Radial velocities and accurate parallaxes will also be necessary to establish the actual spatial and temporal extent of this putatively giant starburst region in our own Galaxy.

Acknowledgements. We thank the referee, Dr. Ben Davies, for his useful suggestions, which led to substantial improvement. We thank Antonio Floría for the enhancement effects in the three-colour image of the cluster. The WHT is operated on the island of La Palma by the Isaac Newton Group in the Spanish Observatorio del Roque de los Muchachos of the Instituto de Astrofísica de Canarias. We thank the ING service programme for their invaluable collaboration. In particular, we thank M. Santander for his support in preparing the observations. This research is partially supported by the Spanish Ministerio de Ciencia e Innovación (MICINN) under grants AYA2008-06166-C03-03 and CSD2006-70, and by the Generalitat Valenciana under grant ACOMP/2009/164. J.S.C. acknowledges support from an RCUK fellowship. S.M.N. is a researcher of the Programme Juan de la Cierva, funded by the MICINN. UKIDSS uses the UKIRT Wide Field Camera (WFCAM; Casali et al. 2007) and a photometric system described in Hewett et al. (2006). The pipeline processing and science archive are described in Hambly et al. (2008). This publication makes use of data products from the Two Micron All Sky Survey, which is a joint project of the University of Massachusetts and the Infrared Processing and Analysis Center/California Institute of Technology, funded by the National Aeronautics and Space Administration and the National Science Foundation.

References

Alexander, M. J., Kobulnicky, H. A., Clemens, D. P., et al. 2009, AJ, 137, 4824
Bastian, N., Gieles, M., Efremov, Yu. N., & Lamers, H. J. G. L. M. 2005, A&A, 443, 79
Benjamin, R. A., Churchwell, E., Babler, B. L., et al. 2003, PASP, 115, 953
Cabrera-Lavers, A., Garzón, F., & Hammersley, P. L. 2005, A&A, 433, 173
Cabrera-Lavers, A., González-Fernández, C., Garzón, F., et al. 2008, A&A, 491, 781
Casali, M., Adamson, A., Alves de Oliveira, C., et al. 2007, A&A, 467, 777
Clark, J. S., Negueruela, I., Crowther, P. A., & Goodwin, S. P. 2005, A&A, 434, 949
Clark, J. S., Negueruela, I., Davies, B., et al. 2009a, A&A, 498, 109
Clark, J. S., Davies, B., Najarro, F., et al. 2009b, A&A, 504, 429
Cotera, A. S., Erickson, E. F., Colgan, S. W. J., et al. 1996, ApJ, 461, 750
Davies, B., Figer, D. F., Kudritzki, R.-P., et al. 2007, ApJ, 671, 781 (D07)
Davies, B., Figer, D. F., Law, C. J., et al. 2008, ApJ, 676, 1016
Egan, M. P., Price, S. D., & Gugliotti, G. M. 2001, BAAS, 34, 561
Elias, J. H., Frogel, J. A., & Humphreys, R. M. 1985, ApJ, 57, 91
Figer, D. F., McLean, I. S., & Morris, M. 1999, ApJ, 514, 202
Figer, D. F., MacKenty, J. W., Robberto, M., et al. 2006, ApJ, 643, 1166
Garzón, F., López-Corredoira, M., Hammersley, P., et al. 1997, ApJ, 491, L31
González-Fernández, C., Cabrera-Lavers, A., Hammersley, P. L., & Garzón, F. 2008, A&A, 479, 131
Groenewegen, M. A. T., Sloan, G. C., Soszyński, I., & Petersen, E. A. 2009, A&A, 506, 1277
Hambly, N. C., Collins, R. S., Cross, N. J. G., et al. 2008, MNRAS, 384, 637
Hewett, P. C., Warren, S. J., Leggett, S. K., & Hogkin, S. T. 2006, MNRAS, 367, 454
Humphreys, R. M., & McElroy, D. B. 1984, ApJ, 284, 565
Joshi, H., Kumar, B., Singh, K. P., et al. 2008, MNRAS, 391, 1279
Indebetouw, R., Mathis, J. S., Babler, B. L., et al. 2005, ApJ, 619, 931
Krabbe, A., Genzel, R., Eckart, A., et al. 1995, ApJ, 447, L95
Lawrence, A., Warren, S. J., Almaini, O., et al. 2007, MNRAS, 379, 1599
Levesque, E. M., Massey, P., Olsen, K. A. G., et al. 2005, ApJ, 628, 973
van Loon, J. Th., Cioni, M.-R. L., Zijlstra, A. A., & Loup, C. 2005, A&A, 438, 273
López-Corredoira, M., Garzón, F., Beckman, J. E., et al. 1999, AJ, 118, 381
Lucas, P. W., Hoare, M. G., Longmore, A., et al. 2008, MNRAS, 391, 136
Majaess, D. J., Turner, D. G., & Lane, D. J. 2008, MNRAS, 390, 1539
Marigo, P., & Girardi, L. 2008, A&A, 469, 239
Marigo, P., Girardi, L., Bressan, A., et al. 2008, A&A, 482, 883
Messineo, M., Davies, B., Ivanov, V. D., et al. 2009, ApJ, 697, 701
Meynet, G., & Maeder, A. 2000, A&A, 361, 101
Nagata, T., Woodward, C. E., Shure, M., & Kobayashi, N. 1995, AJ, 109, 1676
Negueruela, I., & Schurch, M. P. E. 2007, A&A, 461, 431
Rathborne, J. M., Johnson, A. M., Jackson, J. M., et al. 2009, ApJS, 182, 131
Rayner, J. T., Cushing, M. C., & Vacca, W. D. 2009, ApJS, 185, 289
Straižys, V., & Lazauskaitė, R. 2009, Balt. Astr., 18, 19
Smartt, S. J., Eldridge, J. J., Crockett, R. M., & Maund, J. R. 2009, MNRAS, 395, 1409
Turner, D. G. 1980, ApJ, 240, 137
Vacca, W. D., Cushing, M. C., & Rayner, J. T. 2003, PASP, 115, 389
Walborn, N. R., Maíz-Apellániz, J., & Barbá, R. H. 2002, AJ, 124, 1601